ELSEVIER

Carbohydrate Research 270 (1995) 11–32

CARBOHYDRATE RESEARCH

Synthesis and conformational analysis of the plant hormone (auxin) related 2-(indol-3-yl)ethyl and 2-phenylethyl β-D-xylopyranosides and their 2,3,4-tri-*O*-acetyl derivatives

Sanja Tomić [a], Bouke P. van Eijck [b], Biserka Kojić-Prodić [a,*], Jan Kroon [b], Volker Magnus [a], Biljana Nigović [a], Goran Laćan [a], Nebojša Ilić [a], Helmut Duddeck [c], Monika Hiegemann [d]

[a] *Rudjer Bošković Institute, P.O.B. 1016, 41001 Zagreb, Croatia*
[b] *Department of Crystal and Structural Chemistry, Bijvoet Centre for Biomolecular Research, Utrecht University, Padualaan 8, 3584 CH Utrecht, The Netherlands*
[c] *Universitaet Hannover, Institut fuer Organische Chemie, Schneiderberg 1B, D-30167 Hannover, Germany*
[d] *Ruhr-Universitaet Bochum, Lehrstuhl fuer Strukturchemie, Postfach 10 21 48, D-44780 Bochum, Germany*

Received 7 June 1994; accepted in revised form 21 December 1994

Abstract

The synthesis, structure analysis by X-ray diffraction and NMR spectroscopy (including also ^{1}H {^{1}H}NOE measurements), as well as molecular mechanics and dynamics of D-xylopyranose conjugates of 2-(indol-3-yl)ethanol (**1**) and 2-phenylethanol (**2**) are described. The per-*O*-acetylated derivatives of 2-(indol-3-yl)ethyl β-D-xylopyranoside (**4β**) and 2-phenylethyl β-D-xylopyranoside (**7β**) were prepared [along with corresponding α-D-isomers (**4α** and **7α**) and 1,2-*O*-orthoacetates (**5,8**)] by Koenigs–Knorr condensation of the aglycone alcohols with 2,3,4-tri-*O*-acetyl-α-D-xylopyranosyl bromide. Glycoside **4β** was deprotected to yield 2-(indol-3-yl) ethyl β-D-xylopyranoside (**6**). The crystal structures of **4β** and **7β** were determined. The crystals of both compounds are monoclinic, space group $P\,2_1$ with $a = 11.985(1)$, $b = 7.317(1)$, $c = 12.428(1)$ Å, $\beta = 93.2(1)°$, $Z = 2$ (**4β**); $a = 5.809(1)$, $b = 19.833(1)$, $c = 8.912(1)$ Å, $\beta = 106.0(1)°$, $Z = 2$ (**7β**). The β-D-xylopyranose rings are in the $^4C_1$ chair conformation. The results of the theoretical

* Corresponding author.

Elsevier Science Ltd.
SSDI 0008-6215(95)00037-2

conformational analysis are compared with the values obtained from the experimental measurements in solid state and solution.

Keywords: Auxin; Xylopyranosides; X-ray diffraction; NMR spectroscopy; NOE; Molecular dynamics

1. Introduction

The biological properties of plant growth regulators and biogenetically related compounds have mostly been rationalized [1–3] in terms of structural data deduced by inspection of mechanical molecular models. We have embarked on using experimental methods such as X-ray structure analysis and NMR spectroscopy to gain more detailed insight into molecular architecture within this group of compounds (e.g. [4–10]), and here focus on the β-D-xylopyranosides of 2-(indol-3-yl)ethanol (**1**; β-D-xylopyranoside = **6**) and 2-phenylethanol (**2**). In these studies, the per-*O*-acetylated derivatives (**4**β and **7**β) were preferred to unprotected glycosides, because of higher stability and better crystallisability. Conformational analysis of free glycoside **6** was then, anchored to that experimental base, performed with molecular mechanics and dynamics. The compound has previously [11,12] been used as a standard in studies on the metabolism of **1**.

Alcohols **1** and **2** are endogenous plant constituents; the former (**1**) can be converted to the phytohormone (auxin), indole-3-acetic acid (IAA) and, moreover, appears to take part in auxin homeostasis [13]. Incompletely characterized conjugated forms of **1** are stored in pine seeds and are utilized during germination [14], presumably as a source of IAA for the rapidly developing seedling. If exogenously applied to plant tissues, **1** is converted to esters and glycosides of which the β-D-glucopyranoside and the β-D-galactopyranoside have been identified [11,12]. The β-D-xylopyranoside is of potential significance as other plant-hormone related compounds form conjugates containing this sugar moiety [15]. Glycosides of **1** can apparently be reutilized for IAA biosynthesis, as suggested by their growth-promoting effect in pea-stem segments [16] and pumpkin hypocotyl explants [17].

2-Phenylethyl β-D-xylopyranoside, and its fully acetylated derivative (**7**β), were primarily included in this study for comparative purposes aimed at assessing the influence of the heterocyclic NH-moiety on the conformation of the 2-(indol-3-yl)ethyl analogues (**4**β, **6**). The conversion of alcohol **2** to phenylacetic acid in plant tissues has not been investigated as thoroughly as the corresponding sequence of reactions in the indole series, although both the alcohol [18] and the acid [19,20] exhibit growth-promoting properties if applied in the appropriate range of concentrations. In fact, 2-phenylethanol has received more attention as an ubiquitous constituent of plant essential oils which contributes to their antiseptic properties. The alcohol inhibits bacteria and DNA viruses (e.g. [21,22]). High concentrations are also toxic to plant cells [23]; endogenous **2** is thus sequestered by compartmentalization and by conjugation with D-glucopyranose and disaccharides (e.g. [24,25]). Conjugates with a number of sugars have been tested, in animal systems, as selective drugs from which antimicrobial concentrations of the aglycone (**2**) is liberated in diseased tissues, or by pathogens, which contain the

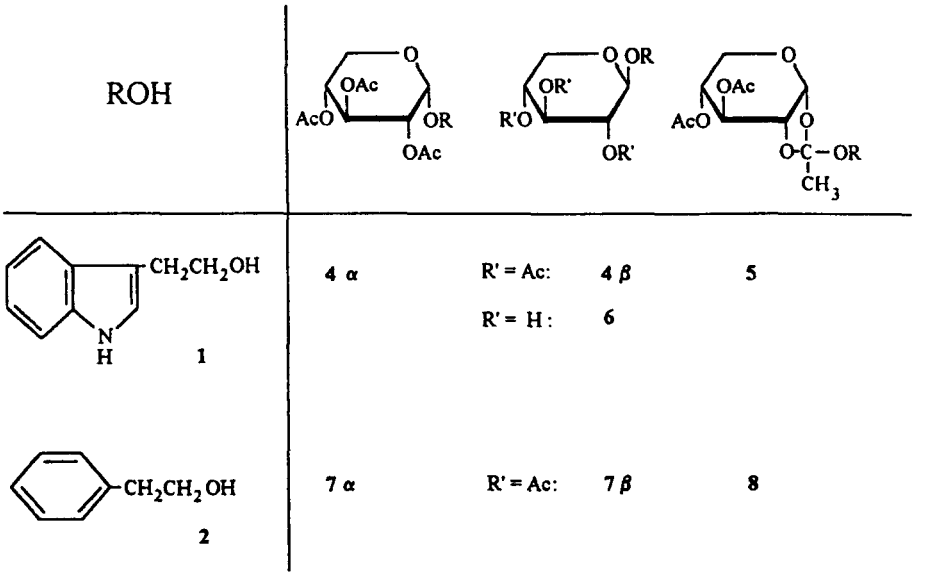

Scheme 1. Chemical formula.

necessary glycosidases (e.g. [26]). As those glycosides per se appear to be inert towards microorganisms, comparison of the molecular structure of the β-D-xylopyranoside to that of free alcohol **2** [27] may shed some light on its mechanism of action which is so far not completely understood [21,22].

2. Results and discussion

Synthesis.—Condensation of 2,3,4-tri-*O*-acetyl xylopyranosyl bromide (**3**) with a 20% molar excess of 2-(indol-3-yl)ethanol (**1**), in the presence of silver oxide and anhydrous calcium sulfate, afforded a mixture of β-D-xylopyranoside (**4β**), the *exo*- and *endo*-isomers of an α-D-xylopyranose 1,2-*O*-orthoacetate (**5**), and, unexpectedly, a minor product with the ^{1}H NMR spectrum [28] of an α-D-xylopyranoside (**4α**). Table 1 summarizes the results of reactions performed in dichloromethane–diethyl ether solutions. The yields of the practically important 1,2-*trans*-D-xylopyranoside (**4β**) were considerably more sensitive to variations in the ratio of the solvent components than previously observed in the L-arabino series [4,29] under identical experimental conditions.

Deprotection of xyloside **4β** afforded the free glycoside **6**, which was used as a standard in screening experiments on the conjugation of alcohol **1** in plant tissues [11,12].

The known [28,30] per-*O*-acetylated 2-phenylethyl xylopyranoside **7β** was here

Table 1
Ratios of per-*O*-acetylated α-D-xylopyranoside (**4α**), β-D-xylopyranoside (**4β**), and α-D-xylopyranose 1,2-*O*-orthoacetates (**5**) formed by condensation of glycosyl halide **3** with 2-(indol-3-yl)ethanol (**1**) in dichloromethane–diethyl ether [a]

Ratio of CH_2Cl_2 : Et_2O	Yield [b] (%) of **4α** + **5** + **4β**	Ratio of **4α** : **5** : **4β**
100:0	66	5:68:27
95:5	67	0:72:28
85:15	68	7:65:28
75:25	68	0:70:30
65:35	69	0:69:31
50:50	54	0:58:42
35:65	73	7:55:38
25:75	41	11:25:64
10:90	32	14:19:67
0:100	43	12:20:68

[a] Glycosyl halide **3** (1.1 mmol) was reacted with alcohols **1** or **2** (1.3 mmol) with all conditions identical except for the solvent ratios (see Experimental section for details).
[b] Based on **3**.

prepared and purified in the same way as its analog **4β**. Switching aglycone alcohols **1** and **2** had no significant effect on the overall yields of Koenigs–Knorr products, and the relative abundance of orthoesters and the presumptive α-D-xylopyranosides (relying, for **4α**, **7α** and **8**, solely upon ^{1}H NMR evidence for identification), as long as the reaction was performed in the same solvent; this is not the case in the L-arabino series [4,29].

X-ray structure analysis of 4β and 7β.—The structures of **4β** and **7β** with the atom numbering are shown in Figs 1 and 2; the ORTEP [31] plots for **4β** and **7β** were drawn

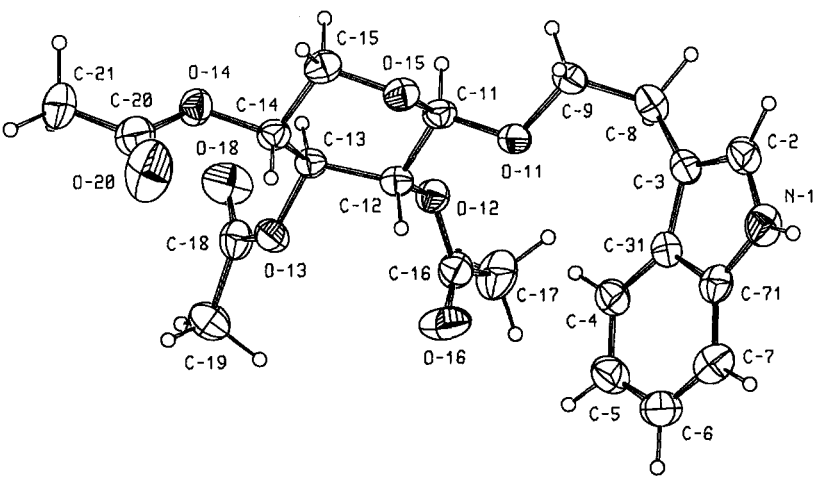

Fig. 1. Molecular structure (ORTEP drawing) of **4β** with atom numbering. The thermal ellipsoids are at the 30% probability level.

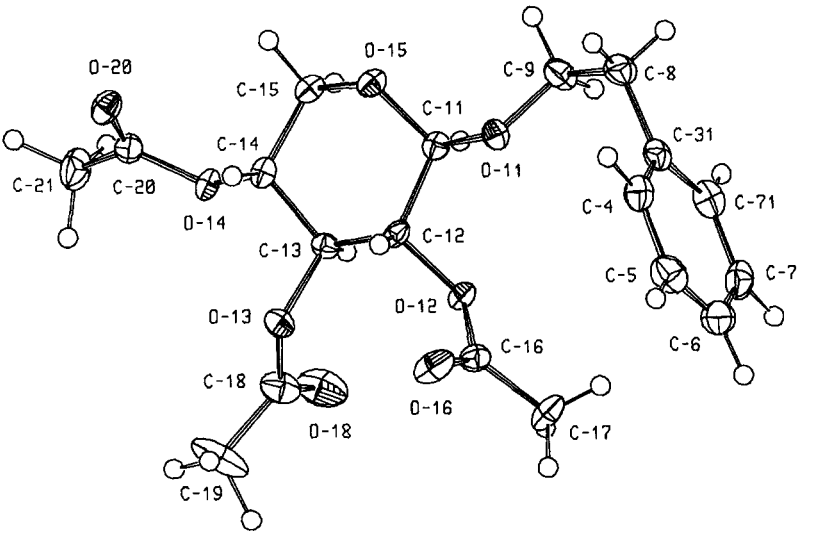

Fig. 2. Molecular structure (ORTEP drawing) of 7β with atom numbering. The thermal ellipsoids are at the 50% probability level.

with thermal ellipsoids at 30% and 50% probability levels, respectively. Bond lengths and angles are listed in Tables 2 and 3. The endocyclic bonds C–O in the xylopyranose ring are equal within the limits of experimental error: C-11–O-15, 1.425(4) Å; C-15–O-15, 1.432(4) Å (4β), C-11–O-15, 1.426(4) Å; C-15–O-15, 1.433(4) Å (7β). The equatorially disposed C-11–O-11 bonds, 1.382(3) Å in 4β and 1.390(4) Å in 7β are significantly shorter than a normal C–O bond (1.428 Å), the effect usually observed for the anomeric C–O bond in equatorial glycopyranosides [32]. The values of the endocyclic angle C-11–O-15–C-15 are 111.6(2)° (4β) and 111.0(2)° (7β). These values are in agreement with the geometry of equatorial glycosidic bonds, typical of β-D-$^4C_1$ pyranosides [32]. The exocyclic valence angle at the glycosidic oxygen in compound 4β is enlarged to 115.6(2)° (7β: 113.8(2)°).

The geometry of the benzene part of indole nucleus in 4β significantly deviates from that of a regular six-membered aromatic ring. Shortening of the C-6–C-7 bond [1.363(8) Å] and shrinkage of the C-6–C-7–C-71 angle [117.9(4)°] were observed in 4β and in many of indole-3-acetic acid derivatives [5] and its amino acid conjugates [6,7], as well as in the previously analysed glycosidic conjugate [4].

The overall molecular conformation is described by selected torsion angles presented in Table 4. According to these values and Cremer and Pople parameters [33] [$\theta = 6.3(3)°$;

Note: The atom numbering of the sugar moiety used in the Experimental section is in agreement with the sugar nomenclature. However, in the X-ray analysis and computational chemistry part an additional digit, being 1, was used in order to be consistent with the indole numbering, employed for the auxin series (e.g. O−5 → O−15).

Table 2
Bond lengths (Å) for **4**β and **7**β

	4β	**7**β
Pyranose moiety		
C-11–C-12	1.508(5)	1.518(5)
C-11–O-11	1.382(3)	1.390(4)
C-11–O-15	1.425(4)	1.426(4)
C-12–C-13	1.509(4)	1.511(5)
C-12–O-12	1.438(3)	1.441(4)
C-13–C-14	1.507(5)	1.511(5)
C-13–O-13	1.447(5)	1.448(4)
C-14–C-15	1.529(6)	1.518(5)
C-14–O-14	1.434(4)	1.442(4)
C-15–O-15	1.432(4)	1.433(4)
O-12–C-16	1.345(4)	1.360(3)
C-16–O-16	1.192(5)	1.199(3)
C-16–C-17	1.507(6)	1.496(5)
O-13–C-18	1.349(4)	1.348(5)
C-18–O-18	1.193(5)	1.204(5)
C-18–C-19	1.489(6)	1.512(6)
O-14–C-20	1.344(6)	1.359(4)
C-20–O-20	1.217(8)	1.202(4)
C-20–C-21	1.485(6)	1.497(5)
Tryptophol moiety		
N-1–C-2	1.368(5)	
N-1–C-71	1.370(6)	
C-2–C-3	1.360(5)	
C-3–C-31	1.436(6)	
C-31–C-71	1.412(4)	
C-31–C-4	1.390(6)	
C-4–C-5	1.370(6)	
C-5–C-6	1.399(6)	
C-6–C-7	1.363(8)	
C-7–C-71	1.407(6)	
C-3–C-8 [a]	1.496(5)	1.512(5)
C-8–C-9	1.497(6)	1.524(5)
C-9–O-11	1.444(5)	1.436(4)
Phenyl		
C-31 → C-4		⟨1.385(5)⟩

[a] C-31–C-8 in **7**β.

$\varphi = 334(3)°$; $Q = 0.584(3)$ Å (**4**β); $\theta = 6.1(3)°$; $\varphi = 359(3)°$; $Q = 0.580(3)$ Å (**7**β)] β-D-xylopyranose rings are in $^4C_1$ chair conformation; the values of endocyclic torsion angles are in agreement with the values found to be standard for β-D-$^4C_1$ saccharides [32]. By inspection of the Cambridge Structural Database [34] on β-D-xylopyranose moiety generally a chair $^4C_1$ conformation was found (eleven hits, eight different compounds); a single example of a twist–boat conformation (^2S_O) for methyl 2,3,4-tri-*O*-benzoyl-β-D-xylopyranoside [35] in the crystal was met with; in solution this com-

Table 3
Bond angles (°) for 4β and 7β

	4β	7β
Pyranose moiety		
C-11–O-15–C-15	111.6(2)	111.0(2)
O-15–C-11–C-12	109.1(3)	109.6(2)
C-11–C-12–C-13	111.6(2)	110.1(2)
C-12–C-13–C-14	110.3(3)	111.3(3)
C-13–C-14–C-15	109.7(3)	110.1(3)
O-15–C-15–C-14	108.2(3)	109.4(2)
C-9–O-11–C-11	115.6(2)	113.8(2)
O-11–C-11–C-12	107.8(2)	108.0(2)
O-15–C-11–O-11	108.2(3)	108.4(2)
O-12–C-12–C-11	108.1(3)	107.2(2)
O-12–C-12–C-13	108.9(2)	108.6(3)
O-13–C-13–C-12	107.3(2)	109.1(2)
O-13–C-13–C-14	108.7(3)	107.4(2)
O-14–C-14–C-13	108.0(3)	105.8(3)
O-14–C-14–C-15	109.3(3)	110.1(2)
Tryptophol moiety		
N-1–C-2–C-3	110.7(3)	
C-2–N-1–C-71	108.7(3)	
C-2–C-3–C-8	124.4(3)	
C-2–C-3–C-31	106.1(3)	
C-3–C-31–C-4	134.9(3)	
C-8–C-3–C-31	129.4(3)	
C-3–C-31–C-71	106.9(3)	
N-1–C-71–C-7	130.3(4)	
N-1–C-71–C-31	107.6(3)	
C-5–C-4–C-31	119.2(4)	120.8(3)
C-4–C-31–C-71	118.2(3)	118.3(3)
C-4–C-5–C-6	122.3(5)	120.4(3)
C-5–C-6–C-7	120.2(5)	120.0(4)
C-6–C-7–C-71	117.9(4)	119.0(3)
C-7–C-71–C-31	122.2(4)	121.5(3)
C-3–C-8–C-9 [a]	116.5(3)	112.8(3)
O-11–C-9–C-8	109.7(3)	107.3(3)

[a] Phenyl ring: C-31.

pound reveals an equilibrium of chair conformations with a proportion of 26% of $^1C_4$ form.

The overall molecular conformations of **4β** and **7β** are determined by the torsion angles about the C-3 → C-11 backbone, i.e. D1(O-15–C-11–O-11–C-9), D2(C-11–O-11–C-9–C-8), D3(O-11–C-9–C-8–C-3*) (sequence for **4β**) (for **7β**: O-11–C-9–C-8–C-31) and D4(C-2–C-3–C-8–C-9) (for **4β**) (sequence for **7β**: C-4–C-31–C-8–C-9) (Table 4). In both structures the side chain is tilted to the aromatic plane: D4 = −109.4(4)° (**4β**) and −115.2(4)° (**7β**). The conformations of the glycosidic torsion angle D1(O-15–C-11–O-11–C-9) are (−)synclinal in **4β** and **7β** (Table 4). The

Table 4
Selected torsion angles (°) for 4β and 7β

	4β	7β
Endocyclic angles		
O-15–C-11–C-12–C-13	55.7(3)	57.0(3)
C-11–C-12–C-13–C-14	−51.6(4)	−51.4(4)
C-12–C-13–C-14–C-15	52.8(3)	51.5(3)
C-13–C-14–C-15–O-15	−59.0(3)	−57.1(3)
C-14–C-15–O-15–C-11	65.6(3)	64.6(3)
C-15–O-15–C-11–C-12	−63.7(3)	−64.6(3)
Exocyclic angles		
C-15–O-15–C-11–O-11	179.3(3)	177.7(2)
O-15–C-11–C-12–O-12	175.5(2)	175.1(2)
C-11–C-12–C-13–O-13	−169.9(3)	−169.8(2)
C-12–C-13–C-14–O-14	171.9(3)	170.5(2)
D1(O-15–C-11–O-11–C-9)	−74.4(3)	−85.7(3)
D2(C-11–O-11–C-9–C-8)	−153.3(3)	−179.8(3)
Tryptophol moiety		
C-4–C-31–C-8–C-9	72.3(5)	
D4(C-2–C-3–C-8–C-9)	−109.4(4)	
D3(O-11–C-9–C-8–C-3)	−71.5(3)	
Phenyl		
C-4–C-31–C-8–C-9[a]		−115.2(4)
O-11–C-9–C-8–C-31[a]		56.7(4)

[a] These torsion angles in 7β are analogous to D4 and D3 in 4β.

conformations in 4β and 7β about the bond of conjugation O-11–C-9 (D2) are (−)antiperiplanar. The torsion angle D3 about C-9–C-8 is in synclinal range (about −70° in 4β and about 60° in 7β) (Table 4).

The peracetylation reduced the number of proton donors in these molecules. In molecule 4β the only proton donor remains is indole N–H which participates in hydrogen bond to endocyclic oxygen atom O-15 (Table 5, Fig. 3) forming an infinite helix along *b*. However, in the crystal structure of 7β the lack of pyrrole NH leaves no possibility for the hydrogen bond N–H · · · O observed in 4β. The crystal packing of 7β is dominated by weak C–H · · · O contacts involving various chemical groups: water molecule and terminal methyl group (C-19) and also methylene groups (C-8, C-9). Water molecule (with population less than 1) can be assigned as the proton acceptor in these interactions. The aromatic C(sp^2) (C-7–H) of benzene ring and pyranose C(sp^3) atoms: C-11–H and C-13–H participate as donors to the acetyl groups in C–H · · · O contacts (Table 5). Recently, more information on this type of contacts and its function appears in the literature [36]. The neutron diffraction data of the crystal structure of vitamin B_{12} coenzyme at 15 K offer more accurate data on C–H · · · O contacts [37].

Molecular mechanics (MM) and molecular dynamics (MD) in vacuo for 4β and 6.—Molecular mechanics (MM) calculations were carried out using the program DISCOVER [38], version 3.1 (Biosym, 1993), with the CVFF [39] force field and by the

Table 5
Hydrogen bonds and C–H · · · O contacts in the crystal structures of compounds **4β** and **7β**

Compound		D · · · A (°)	D–H (Å)	H · · · A (Å)	D–H · · · A (°)	Symmetry operations on A
4β	N-1–H · · · O-15	3.013(4)	0.93(4)	2.13(4)	159(3)	$-x+2, 1/2+y-1, -z+1$
	C-19–H · · · O-14	3.544(5)	1.08(5)	2.57(5)	150(4)	$-x+1, 1/2+y, -z$
7β	C-11–H · · · O-20	3.439(4)	1.01(3)	2.56(3)	144(2)	$x-1, y, z$
	C-13–H · · · O-20	3.274(4)	0.90(2)	2.51(3)	143(2)	$x-1, y, z$
	C-7–H · · · O-16	3.404(5)	0.99(4)	2.58(4)	141(3)	$x-1, y, z$
	C-19–H · · · O(H_2O)	2.92(2)	0.97(6)	2.18(6)	132(5)	x, y, z
	C-9–H · · · O(H_2O)	3.25(2)	1.03(3)	2.59(4)	122(2)	$-x+1, 1/2+y-1, -z$
	C-8–H · · · O(H_2O)	3.27(2)	0.98(3)	2.49(3)	137(2)	$-x, 1/2+y-1, -z$

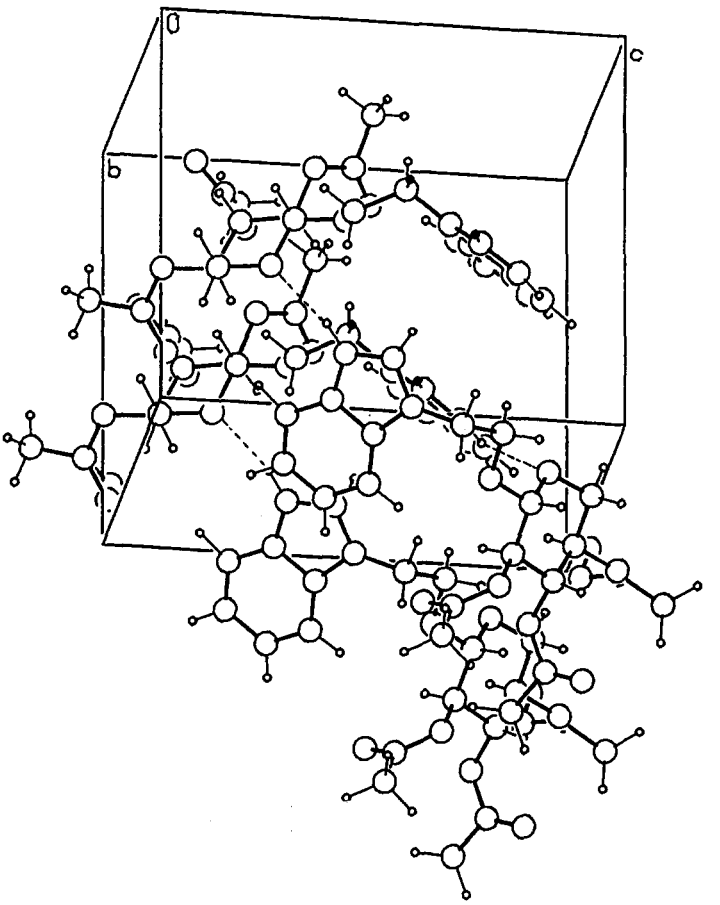

Fig. 3. Molecular packing of **4**β.

MM2(87) [40,41] computer program. In the MM2(87) force field new torsion parameters for N (pyrrole type) have been used [42]. The results obtained with these two programs are in accord. During the minimization of the crystallographically determined structure of **4**β the torsion angles D1–D4 remained in their previous conformations: (−)synclinal (sc), antiperiplanar (ap), (−)synclinal and (−)anticlinal (ac). A systematic search of the conformational space was performed by simultaneous rotations (in 15° and 10° steps) about two pairs (D1–D2 and D3–D4) of the relevant bonds (DISCOVER-CVFF) given in the atom sequences for D1–D4, (Table 4). The conformation of the remaining part of the molecule was kept fixed as determined by X-ray diffraction analysis. The results can be summarized as follows: there are six broad minima on the D4, D3 contour graph [Fig. 4(a), the areas: A, B, C, D, E and F], and two broad accessible regions on the D2, D1 contour graph [Fig. 4(b): hatched regions 1 and 2]. The most favourable conformations about the anomeric bond (D1) are (−)sc and (+)sc. About the bond O-11–C-9 a range

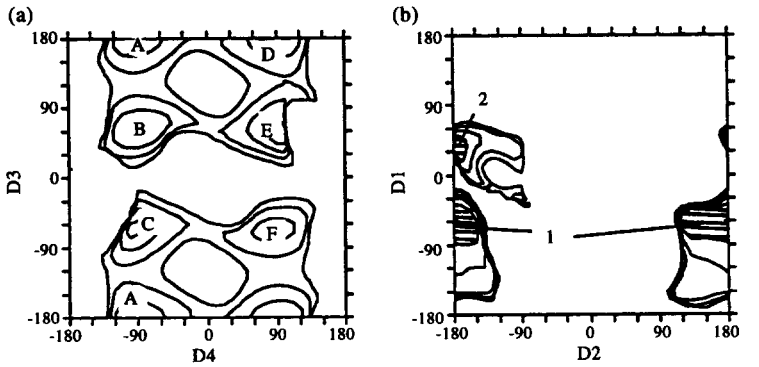

Fig. 4. Two-dimensional energy maps for **4**β as a function of the two torsion angles (CVFF): (a) D4 and D3, with D1 (−)synclinal, D2 antiperiplanar; (b) D2 and D1, with D3 (−)synclinal, D4 anticlinal; [D1(O-15–C-11–O-11–C-9), D2 (C-11–O-11–C-9–C-8), D3 (O-11–C-9–C-8–C-3), D4 (C-2–C-3–C-8–C-9)]. Angles are given in degrees (°). The minima on plot (a) are labelled with letters A–F, and on plot (b) by numbers 1,2 (hatched regions). Contour lines are drawn at an interval of 2 kcal mol^{-1}.

of conformations is possible with D2 in the interval (90°, 270°). For D3 all three staggered conformations occur, whereas the torsional angle D4 is either +90° or −90°. The barrier heights between each pair of conformation families: B and E; C and F; A and D [Fig. 4(a)] are about 4 kcal mol^{-1}. The same systematic search was performed for the free glycoside **6**, and almost indentical results are obtained, which means that acetyl groups do not influence the global conformation of the glycoside. During molecular dynamics (MD) simulations of **6** in vacuo (600 ps, DISCOVER-CVFF) the indole plane remained perpendicular to the bond C-8–C-9 [Fig. 5(a)] as it was found in the previously analysed arabinoside conjugate of tryptophol [4] and in the majority of indole-3-acetic acid derivatives [5] and amino acid conjugates [6,7]. The rotations about the C-8–C-9

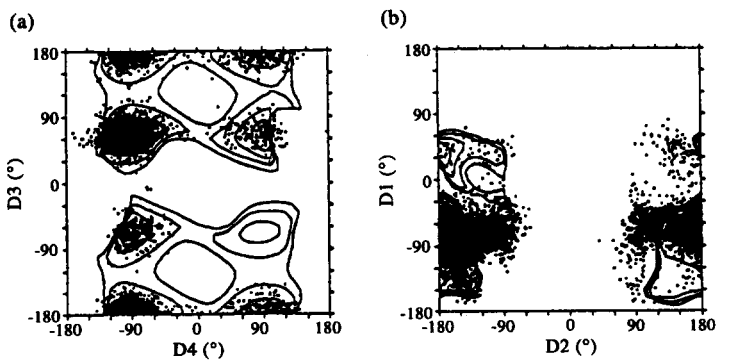

Fig. 5. MD simulations for **6** in vacuo (DISCOVER-CVFF) at room temperature (600 ps). Values of torsion angles (°) D1–D4 obtained during simulations are superimposed on contour graphs from Fig. 4: (a) D4 and D3; (b) D2 and D1.

Table 6
Energy minimized conformations of **6** detected during MD simulations in vacuo (DISCOVER-CVFF)

Torsion angles (°)	The closest minima region [a] (D1,D2,D3,D4)	ΔE_{conf} (kcal mol^{-1})
X1 (−62, 176, −68, −97)	(C,1)	2.5
M1 (−77, 180, −62, −96) [b]	(C,1)	
X2 (−64, 178, −69, 85)	(F,1)	2.8
X3 (−66, 179, 180, −98)	(A,1)	1.6
X4 (−74, −168, 63, −95)	(B,1)	1.5
X5 (−57, 126, −71, −93)	(C,1)	2.2
X6 (−67, −84, −56, −78)	(C,1)	1.5
X7 (−75, −160, 64, 94)	(E,1)	0
X8 (42, 148, −65, −89)	(C,2)	0.6
X9 (−68, −90, −178, −93)	(A,1)	2.6
X10 (−65, 180, 180, 93)	(D,1)	1.5
X11 (46, 140, −58, 100)	(F,2)	0.3
X12 (38, 176, 180, 97)	(D,2)	3.5

[a] See Figs 4 and 5.
[b] M1 is X-ray conformation (acetyl groups replaced by hydroxyl) optimized by MM2(87).

bond can be accomplished at room temperature easily if the simulation time is long enough (at least a few tenth ps). MD simulations of **6** in vacuo revealed all three staggered conformations for D3. The variations of dihedrals D3 and D4 occur simultaneously and changes of D3 from (−)sc to (+)sc are accompanied with changes of D4 from (−)ac to (+)ac. The most frequent conformations of D3 and D4 during MD simulations in vacuo are: (sc,ac), (−sc,− ac) and (ap,± ac) as can be seen in Fig. 5(a), where the results of the MD simulations of **6** are superimposed on the contour graphs determined for **4**β. During MD simulations transitions for D1 from $\approx -60°$ to $\approx 45°$ and transitions for D2 from (−)ap [or (−)ac] to ac (ap) were detected [Fig. 5(b)]. The conformers of **6** with sc conformations of D1 have most of the time D2 about 150° [Fig. 5(b)]. Finally, complete energy minimization was performed for the same (representative) conformers obtained during MD simulations and the results are given in Table 6.

MD simulations in water for **6**.—To simulate natural conditions and to evaluate the influence of solvent on the conformational behaviour of compound **6**, an MD study was performed in periodic boxes of water. Simulations were carried out using the DISCOVER [38] and the GROMOS [43] computer programs with a cube ($a = 20$ Å) and a truncated octahedron ($a = 18.5$ Å), as periodic boxes, respectively. The simulations by DISCOVER were performed with CVFF, using the explicit image model, with cut off distances of 19 and 13 Å. The GROMOS simulations were performed using the minimum image model with a cut off distance of 9 Å.

Before simulations, the systems were subjected to steepest descent minimization to relieve unfavourable interactions. After 5 ps of equilibration the systems were simulated for a longer period (≈ 200 ps) at room temperature or to make conformational transitions easier, at elevated temperature [in steps of: (a) 50 K up to 650 K (GROMOS);

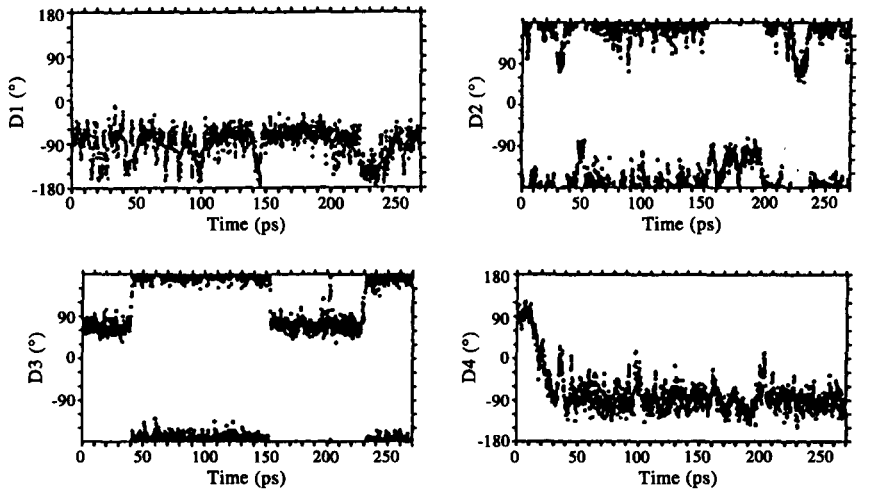

Fig. 6. MD simulations for **6** (initial conformation is X7, see Table 6), in water (DISCOVER-CVFF) at room temperature; variations and torsion angles (°) D1–D4 are given.

(b) 30 K up to 390 K (DISCOVER)]. Water exerts a damping force on the conformational changes, specially when a relatively stable conformation is achieved. To overcome this effect and large flexibility of the molecule, simulations were also carried out starting from different initial solute conformations. Two of these simulations, starting from X7 and X3 conformations (see Table 6) are shown in Figs 6 and 7, respectively. During these simulations the xylopyranoside ring remained in the most stable chair $^4C_1$ conformation. At the temperatures above 650 K the transitions of the sugar ring from $^4C_1$ to $^1C_4$ occurred. After the fast cooling, and further simulations at room temperature, the sugar ring retains its $^1C_4$ conformation.

The conformation determined as global minimum in vacuo (X7, see Table 6) did not remain stable during the (280 ps) simulation in water at room temperature. After ≈ 15 ps the rotation about the C-3–C-8 bond occurred and conformation of D4 slowly changed from +ac to −ac. The rotation about the bond C-8–C-9 followed (after ≈ 40 ps) and D3 changed from sc to ap (Fig. 6).

The results of MD simulations performed in water can be summarized as follows: the conformation of D1 was mostly (−)- or (+)synclinal although transitions of D1 from −sc to (−ac) ap were frequent. The conformation of the D2 was either ap and (±)ac although sc conformations (+sc and −sc) were also detected during simulations. The torsion angle D3 was either around −60°, +60° or 180°, as it was also noticed during MD simulations in vacuo. The torsion angle D4 was either about −90° or +90°.

Conformation of 4β in solution.—In conformationally flexible molecular systems ^{1}H{^{1}H}NOE experiments produce responses for all conformers with reasonable populations [44]. Therefore in a molecule as mobile as those under discussion a great number of NOEs may occur which are not necessarily consistent with one single structure. Nevertheless, it was possible to extract some pieces of evidence which confirm the above X-ray and the MD results.

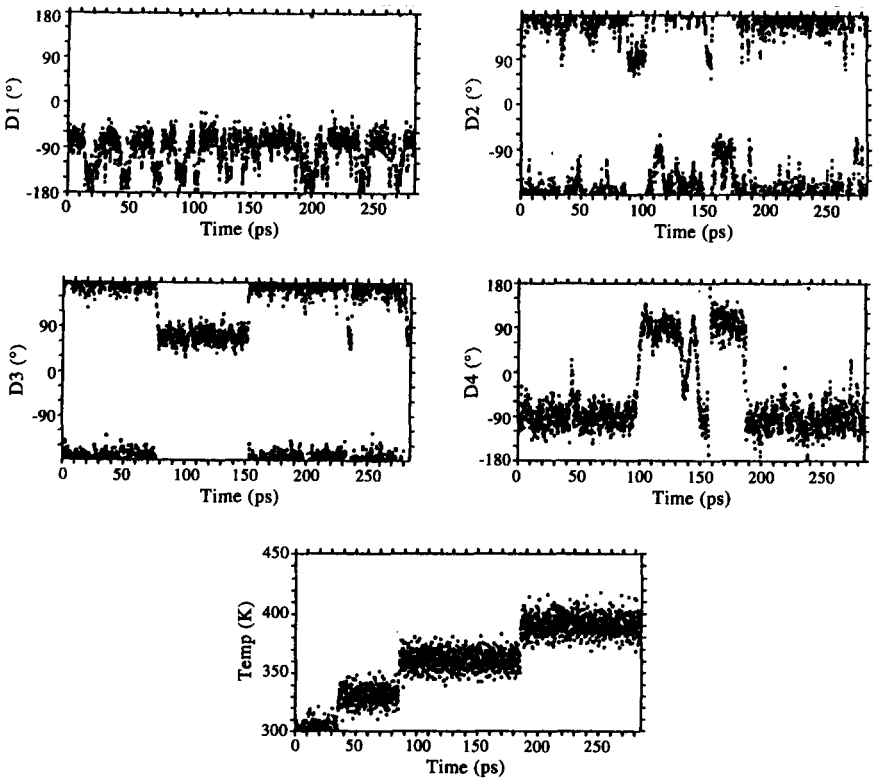

Fig. 7. MD simulations for **6** (initial conformation is X3, see Table 6), in water (DISCOVER-CVFF), at elevated temperature; variations of torsion angles (°) D1–D4 and temperature are given.

According to our measurements the two diastereotopic H-9 atoms (H-9a at $\delta = 4.14$ and H-9b at $\delta = 3.75$) are in rather different spatial orientations with respect to the anomeric hydrogen H-11. Whereas for H-9a the mutual NOE responses are rather low (5.8%, H-11 → H-9a; 1.8%, H-9a → H-11), those for H-9b are very significant (13.6%, H-11 → H-9b; 9.9%, H-9b → H-11). In addition, there are moderate NOE responses for H-11 and one or both of the two diastereotopic but isochronous H-8 signals (6.1%, H-11 → H-8; 3.3%, H-8 → H-11). This is consistent with a tilted antiperiplanar chain from the atom C-11 to C-8; the corresponding torsion angle in the X-ray structure is −153.3° (Table 4). Moreover, it allows to assign the two H-9 atoms: H-9a pro-*S* and H-9b pro-*R*. NOE enhancements between 3.8 and 4.8% are observed between the H-8 signal and those of H-2 and H-4. This agrees with the torsion angle D3 determined by X-ray (−71.5°, Table 4). The absence of strong NOEs between H-9a and H-2 or H-4 (1.2 to 3.3%) supports this conformation which is also in accordance with the MD results.

Conformation of 7β in solution.—The results of the NOE experiments regarding the conformation of the OCH_2CH_2 with the attached β-D-xylose moiety are similar to those

observed for **4**β, and this agrees again with the X-ray findings. A significant NOE response (6.4%) appears at the *ortho*-proton signals of the phenyl ring where H-8 is irradiated, but this does not indicate a preference in the conformational behaviour of the aromatic ring.

3. Conclusions

The comparison of the results from X-ray diffraction analysis, MM (CVFF and MM2(87) force fields) and MD (DISCOVER-CVFF and GROMOS) with the results obtained previously for the arabinoside conjugate of tryptophol [4], the galactoside conjugate of tryptophol and the glucoside conjugate of indole-3-acetic acid [8] leads to the conclusion that water does not influence significantly the conformation of the molecules, although some minor differences were noticed. The findings of Hardy and Sarko for cellobiose [45] are similar. The simulations in water, described in this work, show that the most frequent conformations in water are those determined as minima during MM calculations (Fig. 4). X-ray diffraction analysis revealed the chair $^4C_1$ conformation of sugar ring in all glycoconjugates analysed [4,8]. Solvent (water) was observed to have minor influence on the ring conformation: the initial chair conformation was maintained during MD simulations at temperatures < 650 K. The torsional angle D4 was about $(\pm)90°$ in all stable conformations of glycoconjugates. The presence of various aromatic systems (indole in **4**β and phenyl in **7**β) in the conjugated molecules has not affected the conformation of D4.

4. Experimental

General.—Analytical samples were dried in vacuo (323 K, 10^{-4} Torr, 3 d). Melting points were determined in open capillaries and are reported uncorrected. Optical rotations were measured with a Zeiss Kreispolarimeter. Routine ^{1}H NMR spectra were recorded at 90 MHz, with a digital resolution of 0.2 Hz, on a JEOL FX-90 Fourier transform spectrometer using Me_4Si as an internal standard. Analytical TLC was performed on silica gel GF (Merck) with detection by UV fluorescence and by spraying with 10% H_2SO_4 in EtOH and heating. Preparative chromatography was accomplished by TLC on silica gel PF_{254} (Merck) or on a column (65×2 cm) containing a mixture of silica gel H (65 g) and celite (40 g) (Kemika, Zagreb, Croatia). The following eluents were used: A (20:3 CH_2Cl_2–diethyl ether), B (10:1 CH_2Cl_2–petrol), and C (8:2 CH_2Cl_2–MeOH). 2,3,4-Tri-*O*-acetyl-α-D-xylopyranosyl bromide (**3**) [46] was prepared by treating a dichloromethane solution of D-xylopyranose tetraacetate [47] with 35% hydrogen bromide in glacial acetic acid [48].

The steady state NOE-difference spectra were measured in $CDCl_3$ at 400.1 MHz (Bruker AM-400) using a standard pulse technique. Details have been described by us before [10]. Longitudinal relaxation times were estimated not to exceed 2 s.

Condensation of 2,3,4-tri-O-acetyl-α-D-xylopyranosyl bromide (3) with 2-(indol-3-yl)ethanol (1) or 2-phenylethanol (2).—Reactions were performed in the dark, at room temperature, in anhydrous CH_2Cl_2–diethyl ether as specified in Table 1. To a vigorously stirred suspension of alcohol **1** or **2** (1.3 mmol), solvent (20 mL), freshly prepared, dry Ag_2O (0.15 g, 0.65 mmol), and anhydrous $CaSO_4$ (0.5 g) was added, in small portions through 1 h, a solution of **3** (stabilized with 5% $CaCO_3$; 1.1 mmol) in the same volume of solvent. The mixture was further agitated for 16 h. Insoluble components were removed by centrifugation, and the supernatant was concentrated in vacuo and immediately passed through a column of silica gel–celite eluted with solvent A to yield, in this order: (a) residual **3**; (b) the presumptive α-D-xylopyranoside (**4α**, **7α**); (c) the orthoesters (**5**, **8**; *exo-* and *endo*-isomers); (d) the β-D-xylopyranoside (**4β**, **7β**). Preliminary identification was by TLC using solvent A [$R_f \sim 0.8$ (**3**) and 0.6–0.7 (condensation products)] and multiple development with solvent B (separates condensation products in the same order as above, with *exo-* and *endo*-orthoesters yielding distinct spots). TLC (solvent A) of the crude reaction mixture also revealed the presence of unconsumed alcohols **1** or **2** ($R_f \sim 0.4$) and of 2,3,4-tri-*O*-acetyl D-xylopyranose ($R_f \sim 0.2$) which were not isolated. Further work-up was as follows.

(a) 2,3,4-Tri-O-acetyl-α-D-xylopyranosyl bromide (3). Typical amounts reisolated following condensation with **1** were (solvent CH_2Cl_2–diethyl ether ratio in parentheses) 7% (0:100) and 0.2% (25:75). Following condensation with **2**, 1–2% of **3** was recovered. Its identity was confirmed by NMR spectroscopy.

(b) 4α preliminarily identified [28] as 2-(indol-3-yl)ethyl 2,3,4-tri-O-acetyl-α-D-xylopyranoside. ^{1}H NMR data ($CDCl_3$): δ 5.05 (d, 1 H, $J_{1,2} = 3.6$ Hz, H-1); 4.80 (dd, 1 H, $J_{2,3} = 9.9$ Hz, H-2); 5.55 (t, 1 H, $J_{3,4} = 9.9$ Hz, H-3); 4.94 (td, 1 H, $J_{4,5a} = 10.3$ Hz, $J_{4,5b} = 5.7$ Hz, H-4); 3.49 (t, 1 H, $J_{5a,5b} = 11.0$ Hz, H-5a); 3.72 (dd, 1 H, H-5b); 1.96, 2.02, 2.05 (3s, 3 × 3 H, 3 OAc); 8.23 (broad s, 1 H, indole NH); 7.05–7.76 (m, 5 H, indole CH); 3.06 (t, 2 H, $J_{vic} = 7.0$ Hz, $ArCH_2$); 3.96 (dt, 1 H, $J_{gem} = 9.4$ Hz, OCH_aH_b); 3.70 (dt, 1 H, OCH_aH_b).

(c) 3,4-Di-O-acetyl-1,2-O-[1-[2-(indol-3-yl)ethoxy]ethylidene]-α-D-xylopyranose (5). Fractions containing the title compound [*exo*-2-(indol-3-yl)ethoxy isomer prevailing] pure shown by TLC and NMR afforded, after drying in vacuo at 40°C, the analytical sample as a white amorphous solid. ^{1}H NMR data ($CDCl_3$): *exo*-isomer: δ 5.34 (d, 1 H, $J_{1,2} = 4.4$ Hz, H-1); ca. 3.9 (part of m, H-2); 5.16 (t, 1 H, $J_{2,3} \sim J_{3,4} = 2.7$ Hz, H-3); ca. 4.8 (m, 1 H, H-4); 3.62 (dd, 1 H, $J_{4,5a} = 6.5$, $J_{5a,5b} = 11.8$ Hz, H-5a); 3.89 (dd, 1 H, $J_{4,5b} = 5.3$ Hz, H-5b); 2.06 (s, 2 × 3 H, 2 OAc); 1.72 (s, 3 H, ethylidene CH_3); 3.01 (t, 2 H, $J = 6.9$ Hz, $ArCH_2$); 3.77 (t, 2 H, CH_2O); 7.66 (broad s, 1 H, NH); 7.0–7.6 (m, 5 H, indole CH); *endo*-isomer (only two intense signals discernible in mixture of isomers): δ 2.10 (s, 3 H, 1 OAc); 1.67 (s, 3 H, ethylidene CH_3). Anal. Calcd for $C_{21}H_{25}NO_8$ (419.42): C, 60.13; H, 6.01; N, 3.34. Found: C, 60.04; H, 6.30; N, 3.05.

(d) 2-(Indol-3-yl)ethyl 2,3,4-tri-O-acetyl-β-D-xylopyranoside (4β). Repeated recrystallization from 35% aqueous ethanol afforded the pure title compound as white crystals, mp 126–129°C, $[\alpha]_D$ −50.4° (c 1.25, $CHCl_3$). ^{1}H NMR data ($CDCl_3$): δ 4.50 (d, 1 H, $J_{1,2} = 6.4$ Hz, H-1); 4.94 (dd, 1 H, $J_{2,3} = 8.8$ Hz, H-2); 5.17 (t, 1 H, $J_{3,4} = 8.7$ Hz, H-3); ca. 5.0 (td overlapped by other signals, 1 H, H-4); 3.32 (dd, 1 H, $J_{4,5a} = 8.6$ Hz, $J_{5a,5b} = 11.7$ Hz, H-5a); 4.11 (dd, 1 H, $J_{4,5b} = 4.8$ Hz, H-5b); 1.89, 2.01, 2.03 (3 s, 3 × 3

H, 3 OAc); 3.02 (t, 2 H, $J_{vic} = 7.0$ Hz, $ArCH_2$); 4.11 (dt, 1 H, $J_{gem} = 9.1$ Hz, OCH_aH_b); 3.75 (dt, 1 H, OCH_aH_b); 7.62 (broad s, 1 H, NH); 7.56 (d, 1 H, H-4), 7.33 (d, 1 H, H-7), 7.18 (dd, 1 H, H-6), 7.09 (dd, 1 H, H-5), 7.02 (d, 1 H, H-2). The analytical sample was obtained by recrystallization from CH_2Cl_2–hexane. Anal. Calcd for $C_{21}H_{25}NO_8$ (419.42): C, 60.13; H, 6.01; N, 3.34. Found: C, 60.39; H, 5.88; N, 3.23.

*(e) 2-Phenylethyl 2,3,4-tri-*O*-acetyl-β-*D*-xylopyranoside (7β).* Recrystallization from aqueous ethanol gave the pure title compound [30]. ^{1}H NMR data ($CDCl_3$): δ 4.46 (d, 1 H, $J_{1,2} = 6.4$ Hz, H-1); 4.90 (dd, 1 H, $J_{2,3} = 8.3$ Hz, H-2); 5.14 (t, 1 H, $J_{3,4} = 8.0$ Hz, H-3); 4.91 (td, 1 H, H-4); 3.32 (dd, 1 H, $J_{4,5a} = 8.6$, $J_{5a,5b} = 11.7$ Hz, H-5a); 4.07 (dd, 1 H, $J_{4,5b} = 5.0$ Hz, H-5b); 1.93, 2.02, 2.04 (3 s, 3 × 3 H, 3 OAc); 7.27 (m, 2 H, *meta*-H), 7.20–7.18 (m, 3 H, *ortho*- and *para*-H); 2.88 (t, 2 H, $J_{vic} = 6.7$ Hz, $ArCH_2$); 4.08 (dt, 1 H, $J_{gem} = 9.4$ Hz, OCH_aH_b); 3.66 (dt, 1 H, OCH_aH_b). Anal. Calcd for $C_{19}H_{24}O_8$ (380.39): C, 59.99; H, 6.36. Found: C, 59.87; H, 6.36.

Table 7
Crystal data and summary of experimental details for **4β** and **7β**

	4β	**7β**
Molecular formula	$C_{21}H_{25}NO_8$	$C_{19}H_{24}O_8 \cdot 1/8H_2O$
M_r	419.4	382.6
Crystal size (mm)	0.5×0.3×0.2	0.4×0.3×0.1
a (Å)	11.985(1)	5.809(1)
b (Å)	7.317(1)	19.833(1)
c (Å)	12.428(1)	8.912(1)
β (°)	93.2(1)	106.0(1)
V (Å^3)	1088.2(2)	989.6(2)
Crystal system	monoclinic	monoclinic
Space group	$P2_1$	$P2_1$
D_x (g cm^{-3})	1.280	1.337
Z	2	2
μ (cm^{-1})	0.92 (Mo-$K\alpha$)	0.98 (Mo-$K\alpha$)
F(000)	444	406
T (K)	295(2)	103(2)
No. of reflections used for cell parameters	25	25
θ range (°) used for cell parameters	7.0–18.0	7.0–17.0
θ range for intensity measurement (°)	2.0–25.0	2.0–25.0
hkl range	(0,14; 0,8; −14,14)	(0,6; 0,23; −10,10)
$\omega/2\theta$ scan	0.79+0.15 tan θ	0.79+0.15 tan θ
No. of measured reflections	2192	1987
No. of symm. independent refl. with $I > 2\sigma(I)$	1818	1807
No. of variables	354	335
R	0.034	0.030
Rw ($w = k/\sigma^2(F_0)$)	0.030	0.028
S	0.32	0.43
Final shift/error	< 0.5	< 0.5
Residual electron density $(\Delta\rho)_{max}$, $(\Delta\rho)_{min}$ (e Å^{-3})	0.11, −0.14	0.16, −0.18

2-(Indol-3-yl)ethyl β-D-xylopyranoside (6).—A solution of **4β** (231 mg, 0.55 mmol) in methanol (10 mL) presaturated with gaseous NH_3 was left (3 h) at room temperature until TLC (solvent C) indicated complete deacetylation. Evaporation of the solvent gave syrupy **6** which was purified by preparative TLC (solvent C, $R_f = 0.3$). The product (132 mg, 82%) was rechromatographed (solvent C) to yield, after drying in vacuo (70°C, 3 d), the analytical sample as a white, amorphous hygroscopic solid, $[\alpha]_D - 9.82$ (c 0.55, 95% EtOH). Anal. Calcd for $C_{15}H_{19}NO_5$ (293.32): C, 61.42; H, 6.53; N, 4.78. Found: C, 61.22; H, 6.58; N, 4.95.

X-ray structure determination of 4β and 7β.—Crystals suitable for X-ray analysis of both compounds were grown from ethanol at about 277 K in the dark for a few days. The crystals of **7β** were unstable at room temperature and data collection was performed at 100 K. The crystal data and summary of the experimental details for both compounds

Table 8
Final atomic coordinates and equivalent isotropic thermal parameters for **4β**

Atom	*x*	*y*	*z*	U_{eq} [a] (Å^2)
O-11	0.7776(2)	0.3250(4)	0.3123(1)	0.0618(8)
O-12	0.5760(1)	0.5127(4)	0.2698(1)	0.0569(7)
O-13	0.6113(2)	0.8554(4)	0.1626(2)	0.0590(8)
O-14	0.7445(2)	0.8069(4)	−0.0219(2)	0.0644(8)
O-15	0.8534(2)	0.46200	0.1693(1)	0.0581(8)
O-16	0.5930(2)	0.7002(5)	0.4115(2)	0.1026(14)
O-18	0.4594(2)	0.8158(5)	0.0522(2)	0.0982(11)
O-20	0.8774(4)	1.0168(14)	0.0125(7)	0.133(3)
O-21	0.8199(13)	1.067(2)	0.0249(14)	0.079(6)
N-1	0.9799(2)	0.0858(6)	0.6553(3)	0.0760(14)
C-2	0.9417(3)	−0.0016(6)	0.5632(3)	0.0724(16)
C-3	0.8602(2)	0.0981(6)	0.5101(2)	0.0565(11)
C-4	0.7783(3)	0.4136(6)	0.5641(3)	0.0676(14)
C-5	0.7878(4)	0.5461(7)	0.6420(4)	0.0829(17)
C-6	0.8623(4)	0.5307(8)	0.7323(3)	0.0858(17)
C-7	0.9307(3)	0.3824(8)	0.7441(3)	0.0773(14)
C-8	0.7990(3)	0.0400(6)	0.4076(3)	0.0688(14)
C-9	0.8247(4)	0.1436(6)	0.3081(3)	0.0661(14)
C-11	0.7517(3)	0.4063(5)	0.2137(2)	0.0535(11)
C-12	0.6816(2)	0.5730(5)	0.2332(2)	0.0507(11)
C-13	0.6610(3)	0.6843(5)	0.1318(2)	0.0491(11)
C-14	0.7698(3)	0.7242(5)	0.0812(2)	0.0529(11)
C-15	0.8337(3)	0.5460(6)	0.0659(3)	0.0628(14)
C-16	0.5423(3)	0.5844(7)	0.3622(3)	0.0684(14)
C-17	0.4346(3)	0.4988(8)	0.3941(3)	0.1008(19)
C-18	0.5082(3)	0.9005(6)	0.1221(3)	0.0641(14)
C-19	0.4676(3)	1.0689(7)	0.1747(3)	0.0864(17)
C-20	0.7950(4)	0.9655(7)	−0.0438(3)	0.0833(17)
C-21	0.7503(4)	1.0359(7)	−0.1497(3)	0.103(2)
C-31	0.8461(2)	0.2596(6)	0.5736(2)	0.0528(11)
C-71	0.9225(3)	0.2466(6)	0.6639(3)	0.0616(14)

[a] $U_{eq} = (1/3)\,\Sigma_i\Sigma_j U_{ij} a_i^* \cdot a_j^* \boldsymbol{a}_i \cdot \boldsymbol{a}_j$.

are listed in Table 7. The X-ray intensity data were collected on an Enraf–Nonius CAD4 diffractometer with Mo-$K\alpha$ radiation. There were no significant variations in intensity for standard reflections. The data were corrected for Lorentz and polarization effects. The structures were solved by the SHELX86 [50] program. During the structure determination of **4**β two positions of carbonyl oxygen O-20, separated by 0.8 Å, are found: with population parameters 0.75 and 0.25 (O-20 and O-21 in Table 8). However, difference Fourier map did not reveal the splits of C-20 and C-21 maxima, expected from twofold disorder. High temperature factors [C-20: $U_{11} = 0.096(3)$, $U_{22} = 0.078(3)$, $U_{33} = 0.078(3)$; C-21: $U_{11} = 0.147(4)$, $U_{22} = 0.089(4)$, $U_{33} = 0.076(3)$] of these atoms are related with disorder. The ORTEP plot includes the atom with $pp = 0.75$. In difference Fourier map of compound **7**β positive electronic density (0.6 e Å^{-3}) was noticed and assigned to the crystalline solvent molecule, detected as water molecule with population parameter < 1.0. The refinement procedure including coordinates and population parameter of water reduced R value from 3.5% to 3.0% and Rw from 3.2% to

Table 9
Final atomic coordinates and equivalent isotropic thermal parameters for **7**β

Atom	x	y	z	U_{eq} [a] (Å^2)
O-11	0.0605(4)	0.0229(1)	0.1494(2)	0.0205(6)
O-12	0.0107(3)	0.1573(1)	0.2303(2)	0.0191(6)
O-13	0.3713(4)	0.2441(1)	0.1534(2)	0.0216(6)
O-14	0.3726(4)	0.2242(1)	−0.1605(2)	0.0207(7)
O-15	0.2387(4)	0.0558	−0.0373(2)	0.0213(7)
O-16	0.2848(4)	0.1568(2)	0.4656(2)	0.0339(8)
O-18	0.0649(5)	0.3181(2)	0.0887(3)	0.0454(9)
O-20	0.7096(4)	0.1842(1)	−0.2054(2)	0.0254(7)
C-4	0.0148(6)	−0.0551(2)	0.4865(4)	0.0277(10)
C-5	−0.0189(7)	−0.0265(2)	0.6205(4)	0.0341(11)
C-6	−0.2282(7)	0.0064(2)	0.6161(4)	0.0347(12)
C-7	−0.4110(6)	0.0097(2)	0.4770(4)	0.0321(11)
C-8	−0.1194(7)	−0.0796(2)	0.1984(4)	0.0280(10)
C-9	−0.1191(6)	−0.0256(2)	0.0771(4)	0.0275(10)
C-11	0.0807(5)	0.0758(2)	0.0519(3)	0.0188(9)
C-12	0.1861(5)	0.1356(2)	0.1535(3)	0.0185(9)
C-13	0.2324(5)	0.1926(2)	0.0535(3)	0.0174(8)
C-14	0.3756(5)	0.1691(2)	−0.0548(3)	0.0197(9)
C-15	0.2592(6)	0.1075(2)	−0.1449(3)	0.0214(9)
C-16	0.0826(5)	0.1650(2)	0.3880(3)	0.0221(9)
C-17	−0.1254(6)	0.1839(2)	0.4477(4)	0.0292(10)
C-18	0.2697(7)	0.3049(2)	0.1555(4)	0.0307(11)
C-19	0.4528(9)	0.3536(2)	0.2502(5)	0.0527(14)
C-20	0.5558(6)	0.2264(2)	−0.2279(3)	0.0229(10)
C-21	0.5381(7)	0.2878(2)	−0.3277(4)	0.0370(12)
C-31	−0.1617(6)	−0.0513(2)	0.3460(3)	0.0228(9)
C-71	−0.3750(6)	−0.0193(2)	0.3437(4)	0.0286(11)
O [b]	0.673(3)	0.4018(2)	0.013(2)	0.036(6)

[a] $U_{eq} = (1/3)\,\Sigma_i\Sigma_j U_{ij} a_i^* \cdot a_j^* \boldsymbol{a}_i \cdot \boldsymbol{a}_j$.
[b] O from the water molecule.

2.8%. Residual density dropped to 0.16 e $Å^{-3}$; population parameter of 0.125 was reached. Refinement was by full-matrix least-squares on F minimizing $\Sigma w(|F_o| - |F_o|)^2$ with the SHELX77 program [51]. The H atom coordinates were determined from the subsequent difference Fourier syntheses. The H atoms attached to the terminal methyl groups (C-17, C-19, C-21) of **4**β were calculated on stereochemical grounds and refined riding on their respective C atoms. Atomic scattering factors were those included in SHELX77 [51]. Details of the refinement procedure are given in Table 7. In the structure determination of xylopyranoside conjugates, the D-enantiomers were selected according to the assignment (R) at the C4 atoms. The molecular geometries were calculated by the program EUCLID [56]. Drawings were prepared by the program PLUTON [52] incorporated in EUCLID and ORTEP [31]. The final atomic coordinates and equivalent isotropic thermal parameters are listed in Tables 8 and 9.

Calculations were performed on a Micro-VAX II and cluster of VAX computers, a CONVEX C-120, and on Silicon Graphics workstations at the University of Utrecht, The Netherlands, and at the X-ray Laboratory of the Rudjer Bošković Institute, Zagreb, Croatia.

Acknowledgments

This work was supported by Ministry of Science and Technology grants Nos. 1-07-179, 1-08-195, and The Commission of the European Communities, Brussels, contract No. CI1*-CT91-0891.

The authors thank Dr D. Keglević, Rudjer Bošković Institute, Zagreb, for valuable comments.

Supplementary material

The observed and calculated structure factors, H-atom coordinates, and anisotropic thermal parameters have been deposited with the Cambridge Crystallographic Data Centre. The data may be obtained, on request, from the Director, Cambridge Crystallographic Data Centre, 12 Union Road, Cambridge, CB2 1EZ, UK.

References

[1] K.V. Thimann, *Hormone Action in the Whole Life of Plants*, University of Massachusetts Press, Amherst, Massachusetts 1977.

[2] T.M. Kaethner, *Nature (London)*, 267 (1977) 19–23.

[3] G.F. Katekar, *Phytochemistry*, 18 (1979) 223–233.

[4] S. Tomić, B.P. van Eijck, J. Kroon, B. Kojić-Prodić, G. Laćan, V. Magnus, H. Duddeck, and M. Hiegemann, *Carbohydr. Res.*, 259 (1994) 175–190.

[5] B. Kojić-Prodić, B. Nigović, S. Tomić, N. Ilić, V. Magnus, Z. Giba, R. Konjević, and W.L. Duax, *Acta Crystallogr. Sect B*, 47 (1991) 1010–1019.
[6] B. Kojić-Prodić, B. Nigović, D. Horvatić, Ž. Ružić-Toroš, W.L. Duax, J.J. Stezowski, and N. Bresciani-Pahor, *Acta Crystallogr. Sect. B*, 47 (1991) 107–115.
[7] B. Kojić-Prodić, B. Nigović, V. Puntarec, S. Tomić, and V. Magnus, *Acta Crystallogr. Sect. B*, 49 (1993) 367–374.
[8] S. Tomić, Ph. D Thesis, University of Zagreb, 1993.
[9] S. Tomić, F.B. van Duijneveldt, L.M. Kroon-Batenburg, and B. Kojić-Prodić, *Croat. Chem. Acta*, in press.
[10] H. Duddeck, M. Hiegemann, M.F. Simeonov, B. Kojić-Prodić, B. Nigović, and V. Magnus, *Z. Naturforsch.*, 44c (1989) 543–554.
[11] G. Laćan, V. Magnus, B. Jeričević, Lj. Kunst, and S. Iskrić, *Plant Physiol.*, 76 (1984) 889–893.
[12] G. Laćan, V. Magnus, S. Šimaga, S. Iskrić, and P.J. Hall, *Plant Physiol.*, 78 (1985) 447–454.
[13] V. Magnus and G. Laćan, in R.P. Pharis and S.B. Rood (Eds.), *Plant Growth Substances 1988*, Proc. 13th Int. Conf. Plant Growth Subst., Calgary, Springer, Berlin, 1990, pp. 360–366.
[14] G. Sandberg, A. Ernstsen, and M. Hamnede, *Physiol. Plant.*, 71 (1987) 411–418.
[15] D.W.S. Mok and M.C. Mok, *Plant Physiol.*, 84 (1987) 596–599.
[16] V. Magnus, *Carbohydr. Res.*, 76 (1979) 261–264.
[17] S. Jelaska, V. Magnus, M. Seretin, and G. Laćan, *Physiol. Plant.*, 64 (1985) 237–242.
[18] I. Ivanova, S. Mikhailova, S. Iordanova, M. Naneva, and Kh. Dilov, *Fiziol. Rast. (Sofia)*, 8 (1982) 64–73.
[19] K.V. Thimann and C.L. Schneider, *Am. J. Bot.*, 26 (1939) 328–333.
[20] F. Wightman and D.L. Lighty, *Physiol. Plant.*, 55 (1982) 17–24.
[21] J. Corre, J.J. Lucchini, G.M. Mercier, and A. Cremieux, *Res. Microbiol.*, 141 (1990) 483–497.
[22] J.J. Lucchini, J. Corre, and A. Cremieux, *Res. Microbiol.*, 141 (1990) 499–510.
[23] J. Nitsan and A. Lang, *Dev. Biol.*, 12 (1965) 358–376.
[24] A.R. Guseva, N.Sh. Sikharulidze, and V.A. Paseshnichenko, *Dokl. Akad. Nauk SSSR*, 223 (1975) 1260–1261.
[25] P.J. Williams, C.R. Strauss, B. Wilson, and R.A. Massy-Westropp, *Phytochemistry*, 22 (1983) 2039–2041.
[26] M.A. Johnston and H. Pivnick, *Can. J. Microbiol.*, 16 (1970) 83–89.
[27] J.M. Bakke, *Acta Chem. Scand. Sect. B*, 40 (1986) 407–410.
[28] A. de Bruyn, M. Anteunis, R. van Rijsbergen, M. Claeyssens, and P. Kovác, *J. Carbohydr. Chem.*, 1 (1982–1983) 301–309.
[29] V. Magnus, D. Vikić-Topić, S. Iskrić, and S. Kveder, *Carbohydr. Res.*, 114 (1983) 209–224.
[30] C.K. de Bruyne and G. van der Groen, *Carbohydr. Res.*, 2 (1966) 173–175.
[31] C.K. Johnson, ORTEPII, Report ORNL-5138, Oak Ridge National Laboratory, Tennessee, 1976.
[32] G.A. Jeffrey, *Acta Crystallogr. Sect. B*, 46 (1990) 89–103.
[33] D. Cremer and J.A. Pople, *J. Am. Chem. Soc.*, 97 (1975) 1354–1358.
[34] Cambridge Structural Database System, version 5.06, Cambridge Crystallographic Data Centre, Cambridge, October 1993.
[35] K. Vangehr, P. Luger, and H. Paulsen, *Chem. Ber.*, 113 (1980) 2609–2615.
[36] G.R. Desiraju, *Acc. Chem. Res.*, 24 (1991) 290–296.
[37] J.P. Bouquiere, J.L. Finney, M.S. Lehmann, P.F. Lindley, and H.F.J. Savage, *Acta Crystallogr. Sect. B*, 49 (1993) 79–89.
[38] BIOSYM (1993) DISCOVER, version 3.1, Biosym Technologies, 10065 Barnes Canyon Rd., San Diego CA 92121, 1993.
[39] A.T. Hagler, S. Lifson, and P. Dauber, *J. Am. Chem. Soc.*, 101 (1979) 5122–5130.
[40] N.L. Allinger, *J. Am. Chem. Soc.*, 99 (1977) 8127–8134.
[41] Quantum Chemistry Program Exchange, No MM2(87), Chemistry Department, Indiana University, Bloomington, Indiana.
[42] J.C. Tai and N.L. Allinger, *J. Am. Chem. Soc.*, 110 (1988) 2050–2055.
[43] W.F. van Gunsteren, GROMOS, Groningen Molecular Simulation Computer Program Package, University of Groningen, 1987.

[44] D. Neuhaus and M. Williamson, *The Nuclear Overhauser Effect in Structural and Conformational Analysis*, VCH Publishers, New York, 1989.
[45] B.J. Hardy and A. Sarko, *J. Comput. Chem.*, 14 (1993) 848–857.
[46] J.K. Dale, *J. Am. Chem. Soc.*, 37 (1915) 2745–2747.
[47] W.E. Stone, *Am. Chem. J.*, 15 (1983) 653–656.
[48] L.J. Haynes and F.H. Newth, *Adv. Carbohydr. Chem.*, 10 (1955) 207–257.
[49] C.S. Hudson and J.K. Dale, *J. Am. Chem. Soc.*, 40 (1918) 997–1001.
[50] G.M. Sheldrick, in G.M. Sheldrick, C. Krueger, and R. Goodard (Eds.), *Crystallographic Computing 3*, Oxford University Press, 1985.
[51] G.M. Sheldrick, SHELX77, Program for Structure Determination, University of Cambridge, 1983.
[52] A.L. Spek, in D. Sayre (Ed.), *Computational Crystallography*, Clarendon Press, Oxford, 1982, p 528.